BULLETIN OF THE CHEMICAL SOCIETY OF JAPAN, VOL. 52 (6), 1588—1596 (1979)

The Electronic Spectra and Nonaqueous Oxidation and Reduction Potentials of Azoxybenzenes, and Their Mutual Correlation

Tanekazu KUBOTA,* Hiroshi MIYAZAKI, Masumi YAMAKAWA,
Kiyoshi EZUMI, and Yoshiko YAMAMOTO
Shionogi Research Laboratory, Shionogi and Co., Ltd., Fukushima-ku, Osaka 553
(Received October 20, 1978)

The near-ultraviolet absorption spectra of various *p,p'*- and *m,m'*-disubstituted azoxybenzenes were recorded in aprotic and protic solvents. The PPP-SCFMO-CI calculation was used in analyzing the spectra and the solvent effect on them. The π-π^* bands of azoxybenzene could be well interpreted on the basis of the electronic structure of benzaldehyde *N*-phenyl oxime (a nitrone). In addition, the half-wave potentials of reduction ($E_{1/2}^{\mathrm{red}}$) and oxidation ($E_{1/2}^{\mathrm{oxd}}$) were also measured in nonaqueous solvents. These electrochemical data and the above spectral data satisfied a good linear relation: $(E_{1/2}^{\mathrm{oxd}}-E_{1/2}^{\mathrm{red}})=k_1\cdot E_{\mathrm{ho}\to\mathrm{lu}}^{\mathrm{UV}}+k_2$, this equation having been previously proposed by us. In the Appendix, we have discussed the physical meaning of the constant term, k_2, from the quantitative standpoint, using a series of alternant hydrocarbons as a typical example. Finally, a good linear relation between the $E_{1/2}^{\mathrm{red}}$ or $E_{1/2}^{\mathrm{oxd}}$ values and the substituent constants was demonstrated and discussed in azoxybenzenes.

So far the electronic spectra and the electronic states of multifarious aromatic amine oxides have been extensively studied experimentally and theoretically in singlet, doublet, and triplet states.1) Various kinds of experimental techniques have also been used in the studies.1) However, as far as we know, there have been only a few discussions of the electronic state of azoxybenzenes (AOB's),2—6) which are classified as one of the aromatic amine oxides. In this report, the electronic spectra and the half-wave potentials of the oxidation ($E_{1/2}^{\mathrm{oxd}}$) and reduction ($E_{1/2}^{\mathrm{red}}$) of various substituted AOB's have been systematically examined from the viewpoint of experimental and theoretical treatments. For the $E_{1/2}^{\mathrm{oxd}}$ and $E_{1/2}^{\mathrm{red}}$ values, the interrelation of the half-wave potentials and the electronic spectra is also discussed.7)

Experimental

Spectral and Polarographic Measurements. The absorption

TABLE 1. SUBSTITUTED AZOXYBENZENES INVESTIGATED, WITH THEIR SYNTHETIC AND PURIFICATION METHODS, MELTING POINTS, AND DIPOLE MOMENTS

Substituent e)	Mp b) °C	Dipole moment (D.U.) c)	Synthesic method a)	Refining method d)
H(=AOB)	37(34.5—35.5)10)	1.93(1.72, 1.57)14)		R
4,4'-[N(CH$_3$)$_2$]$_2$	249—250(252)11)		B	R
4,4'-(OCH$_3$)$_2$	119.5—120.5(116.5—118.5)10)			R
4,4'-(OC$_2$H$_5$)$_2$	138—139			R
4,4'-(CH$_3$)$_2$	71.0—71.5(66—68)10)		A	R
4,4'-Cl$_2$	157.5—157.8(154—156)10)	1.76	A	T
4,4'-(COOC$_2$H$_5$)$_2$	115.5—116.0		C	R
4,4'-(CN)$_2$	227.5		C	AC
4,4'-(NO$_2$)$_2$	194.5—195(190—192)12)		C	TR
m,m'-(OCH$_3$)$_2$	53.0—53.5	2.66	A	R
m,m'-(CH$_3$)$_2$	35.0—35.5(33—35)10)		A	R
m,m'-Cl$_2$	98.5—99.0(95.5—97)10)		A	R
m,m'-(COOC$_2$H$_5$)$_2$	80.5—81.0		C	R
m,m'-(CN)$_2$	134.5—135.5		C	R
3,3'-(NO$_2$)$_2$	149(143)3)	4.74		T

a) The compounds designated by A, B, and C were synthesized according to Refs. 10, 11, and 12 in the text respectively. The others were commercially available. b) The melting points are uncorrected. The values in parentheses were taken from the literature in the text. c) Measured at 25 °C in dioxane.13) The values in parentheses were taken from Refs. 14a (1.57: 27 °C, benzene) and 14b (1.72: 22 °C, benzene). d) R: Recrystallized from ethanol except for *m,m'*-(CN)$_2$ and 4,4'-[N(CH$_3$)$_2$]$_2$, where benzene and chloroform were suitable as the solvents respectively. T: Purified by preparative thin-layer chromatography. For 4,4'-Cl$_2$ it was developed with heptane and then recrystallized from ethanol. For 3,3'-(NO$_2$)$_2$, benzene was used for both the development and the recrystallization. AC: Alumina column chromatography was used for 4,4'-(CN)$_2$. Elution was made first with benzene and then with a benzene(1)–ether(1) mixture, the latter portion being recrystallized from ethanol. TR: Although purification was tried repeatedly by thin-layer chromatography (TLC) and by recrystallization for this compound, its purity was not sufficient judging from the TLC and the elemental analyses. Its purity, however, may be about 95%. e) See text and Ref. 50.

spectra were recorded in the usual manner with a Beckman DK-2A Far-UV spectrometer at room temperature. The organic solvents used were CCl_4, CH_2Cl_2, CH_3CN, heptane, ethanol, and methanol, all of which were spectrograde in purity. They were desiccated sufficiently with a suitable drying agent, such as $CaCl_2$, Na, or Mg ribbon, and then carefully rectified.[1b,d] The electrochemical data were obtained using the polarographic technique, whose details have been described in a previous paper.[7a] The DC and AC polarograms were measured with a Yanagimoto polarograph, Model P8-AP (three-electrode system), a saturated calomel electrode (SCE) being used as the reference electrode. The capillary used for the dropping mercury electrode to yield the $E_{1/2}^{red}$ was: $m=0.855$ mg/s and $t=5.17$ s at $h=70$ cm in distilled water at an open circuit. Alternatively, the $E_{1/2}^{oxd}$ values were obtained with a rotating platinum electrode, the type and the manipulation of which are exactly the same as in our previous report.[7a] All the experiments were carried out at 25±0.1 °C in *N*,*N*-dimethylformamide (DMF) or CH_3CN containing 0.1 mol dm^{-3} terapropylammonium perchlorate (TNPAP). The method used in the purification of DMF, CH_3CN, and TNPAP was also the same as in our references.[7a,8,9]

Samples. The substances employed here are listed in Table 1 along with their synthetic and purification methods and the melting points. The compounds whose preparation method and physical constants have not yet been reported were synthesized and purified by applying the methods of similar substances known already (see Table 1). The structure and purity of the samples were checked by means of TLC, IR, UV, dipole moment, and elemental analyses. A good agreement was obtained between the calculated and experimental values of elemental analyses except for the 4,4′-dinitroazoxybenzene, the purity of which is less than the others. The structure of the AOB's synthesized here is well known to be the *trans*-in plane-form, just like [I].

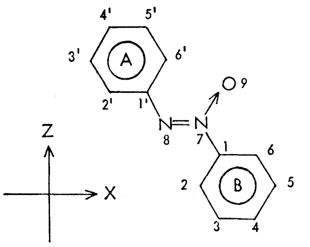

[I]

For the *m*,*m*′-derivatives, however, we could not determine any accurate configuration[50] except for the dinitro derivative, whose NO_2 groups are judged to be in the 3 and 3′ positions from a comparison of the observed (see Table 1) and calculated dipole moments. The latter value is 5.31D, as the vector sum of 1.93D (AOB, whose moment is assumed to be in the direction of the N→O σ moment) and the NO_2 group moment (3.98D)[15] at the 3 and 3′ positions. If two NO_2 groups are in the 5 and 5′ positions, the calculated value is 8.62D.

Results and Discussion

Electronic Spectra of Azoxybenzene Derivatives. As a typical example, the spectrum of AOB is shown in Fig. 1 and compared with that of benzaldehyde *N*-phenyl oxime (BANO: a kind of nitrone),[16] since these are isoelectronic in π-electron systems. It can easily be understood from the figure that the spectra of AOB and BANO are quite similar to each other, especially for the characteristic strong π-π* band appearing in the longest wavelength region, although the bands in the 275—217 nm region is more clearly separated for AOB. This spectral behaviour is very reasonable, as the molecules are the *trans*-in plane-form for both the benzene rings,[17] and suggests that the electronic spectra and the electronic structures of AOB's can be interpreted on the basis of those of BANO previously reported (*vide infra*).[3,16] In the spectra of various substituted AOB's, the spectral pattern of the compounds with electron-donating or electron-accepting substituents at the *p*,*p*′-positions is quite similar to that of AOB, as may be seen in Fig. 2 for 4,4′-bis(dimethylamino)-AOB.

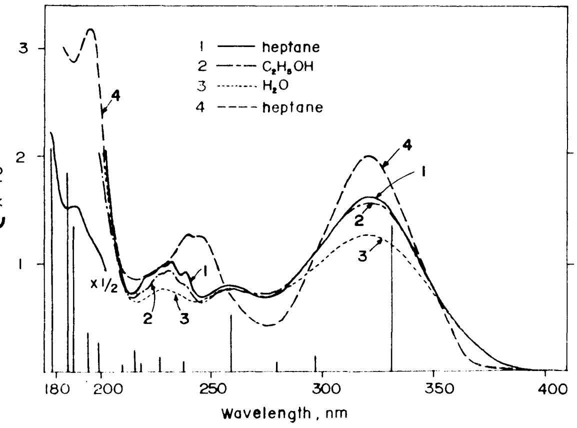

Fig. 1. Electronic spectra of azoxybenzene in aprotic (curve 1) and protic (curves 2 and 3) solvents and of benzaldehyde *N*-phenyl oxime (curve 4) in heptane.

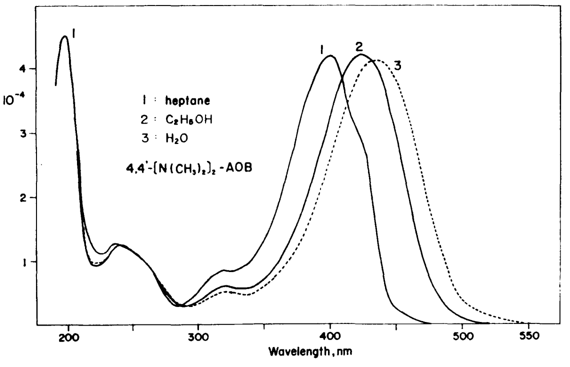

Fig. 2. Electronic spectra of 4,4′-bis(dimethylamino)-azoxybenzene in aprotic (curve 1) and protic (curves 2 and 3) solvents.

For the case of *m*,*m*′-substituents, the weak electron-donating groups like CH_3 and Cl lead also to spectra analogous to that of AOB. On the other hand, if the groups showing quite a large substituent effect are introduced in the *m*,*m*′-positions of AOB, the spectral patterns become very different from that of AOB, as may be understood from Fig. 3. The spectral data are collected in Table 2. Alternatively, the main difference in the spectral behaviour of AOB and BANO is that the well-known blue-shift phenomena found in protic solvents on aromatic amine *N*-oxides including nitrones and nitrile *N*-oxides[18] could not be generally observed

TABLE 2. SPECTRAL AND POLAROGRAPHIC DATA AND SUBSTITUENT CONSTANTS ON VARIOUS SUBSTITUTED AZOXYBENZENES

Compound[j]	First π-π^* band[a]			First wave[b]				First wave[b,e]			Substituent constant[g]	
	λ_{max} (nm)	ε_{max}	$\Delta\tilde{\nu}$[c] (cm^{-1})	$E^{red}_{1/2}$ (volt)[d]	$E^{red}_{1/2}$ (volt)[e]	I_{DC}[d] (μA/mol m^{-3})	I_{AC}[d] (μ℧/mol m^{-3})	$E^{oxd}_{1/2}$ (volt)	I_{DC} (μA/mol m^{-3})	I_{AC} (μ℧/mol m^{-3})	σ	σ^+
AOB	321.5	16050	−50	−1.396	−1.413	2.28	541	2.028	20.7	175	0	0
4,4′-$(CH_3)_2$	330.3	19620	+120	−1.490	−1.505	2.19	575	1.835	18.7	216	−0.170	−0.311
4,4′-Cl_2	333.2	21370	−150	−1.226	−1.260	2.36	589	2.055	14.5	190	0.227	0.114
4,4′-$(OCH_3)_2$	350[h]	23780	+700	−1.596	−1.586	2.04	508	1.463	17.7	298	−0.268	−0.778
4,4′-$(OC_2H_5)_2$	349.5	26910	+690	−1.586	−1.605	2.06	489	1.446	16.8	281	−0.250	—
4,4′-$[N(CH_3)_2]_2$	400.3	40640[f]	+1390	−1.766	−1.748	2.00	439	0.757	11.3	532	−0.600	−1.78
4,4′-$(CN)_2$	334.8	18350[f]	−320	−0.844	−0.900	2.19	541	2.382	16.5	164	1.00[i]	0.659
4,4′-$(COOC_2H_5)_2$	335.5	22180	−160	−0.969	−1.025	2.09	514	2.272	16.1	76	0.678[i]	0.482
4,4′-$(NO_2)_2$	—	—	—	−0.615	−0.705	2.55	307	2.467	20.9	183	1.270[i]	0.790
m,m′-$(CH_3)_2$	324.6	16120	−80	−1.425	−1.435	2.31	551	1.962	16.8	146	−0.069	−0.066
m,m′-Cl_2	322.8	15410	−170	−1.133	−1.183	2.24	565	2.198	22.8	186	0.373	0.399
m,m′-$(OCH_3)_2$	320.0	14090	+40	−1.364	−1.382	1.93	523	1.760	11.1	126	0.115	0.047
m,m′-$(CN)_2$	320.4	16560	−70	−1.001	−1.060	2.22	518	2.350	26.6	172	0.56	0.562
m,m′-$(COOC_2H_5)_2$	321.7	15920	+70	−1.191	−1.234	1.79	435	2.280	22.1	125	0.398	0.366
3,3′-$(NO_2)_2$	316.4	15380	−30	−0.930	−0.947	2.24	438	2.423	29.2	189	0.710	—

a) Data in heptane. b) Data *vs.* S.C.E. c) $\Delta\tilde{\nu}=\tilde{\nu}$ (heptane) − (ethanol). d) Obtained with a dropping mercury electrode in DMF. e) Obtained with a rotating platinum electrode (ϕ = 1 mm, 600 rpm) in CH_3CN. f) Values in CH_3CN. g) Taken from Refs. 7a, 8, 45, and 46 given in the text. h) The symmetry of this absorption curve is bad. The 350 nm is the weighted mean wavelength (center of gravity) of the curve, but the peak is 345.4 nm. i) This is a σ^- value (Jaffé's σ^*) cited from Ref. 47. j) See text and Ref. 50.

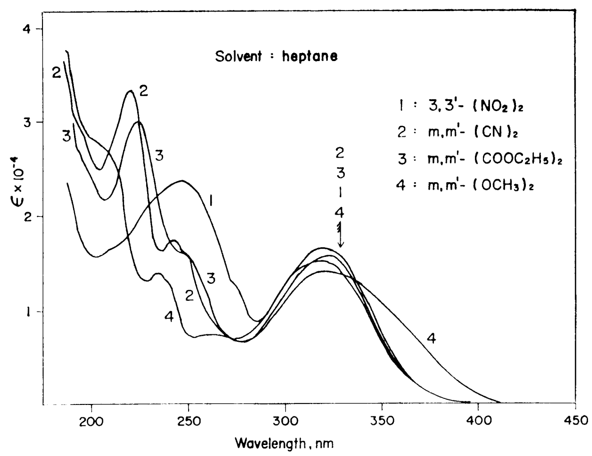

Fig. 3. Electronic spectra of azoxybenzenes substituted at *m,m′*-positions with the groups showing quite a large substituent effect.

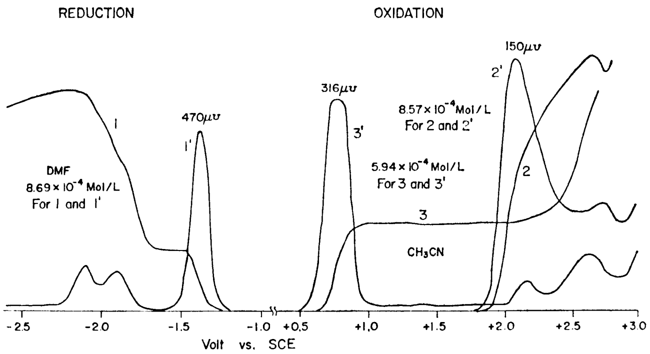

Fig. 4. DC(1) and AC(1′) reduction polarograms in DMF and DC(2) and AC(2′) oxidation voltammograms in CH_3CN of azoxybenzene respectively. Curves 3 and 3′ are DC and AC voltammograms of 4,4′-bis(dimethylamino)azoxybenzene respectively. The absolute value of current is taken at the ordinate for the conveniences's sake.

for AOB and its derivatives. The red shift, rather than the blue shift, of the strong π-π^* band in the longest-wavelength region was observed in protic solvents in the case of substituted AOB's. This red shift is especially large for the AOB's with 4,4′-$[N(CH_3)_2]_2$ (2003 cm^{-1}), 4,4′-$(OC_2H_5)_2$ (976 cm^{-1}), and 4,4′-$(OCH_3)_2$ (949 cm^{-1}): the values in parentheses are the red shift from heptane to aqueous ethanol (C_2H_5OH: H_2O = 3: 2). The spectral change with protic solvents is illustrated in Fig. 2 for the AOB substituted with 4,4′-$[N(CH_3)_2]_2$. The mechanism of the effect of protic solvents on the π-π^* band seems to be more or less different between $-N{=}N{\rightarrow}O$ and $-C{=}N{\rightarrow}O$ groups, the former having two active sites for intermolecular hydrogen-bonding interaction.

Nonaqueous Polarograms and Half-wave Potentials of Reduction and Oxidation. In Fig. 4 are illustrated the reduction polarogram in DMF and the oxidation voltammogram in CH_3CN on AOB as an example. The first reduction wave in Fig. 4 is due to the formation of the corresponding anion radical in the reversible process. This was inferred from the high value (541 μ℧/mol m^{-3}) of the AC wave, and directly verified by recording the ESR spectrum at the potential of the first limiting current. The same circumstances as the above can be applied to the substituted AOB's, the first wave of which is quite a bit similar to that of AOB in showing a high AC wave. Almost the same reduction DC and AC waves which were obtained with a dropping Hg electrode were also yielded with a rotating Pt electrode. These first waves may be attributed to the anion radical formation. The data are listed in Table 2. On the other hand, the first oxidation wave of AOB, depicted in Fig. 4, seems not only to be overlapped with the next waves, but also the reversibility is less[19] than in the case of the reduction wave. The AC waveheight (175 μ℧/mol m^{-3}) is considerably smaller than that (*vide supra*) of the reduction wave. Of the AOB derivatives, 4,4′-bis(dimethylamino)-AOB showed a typical oxidation wave. The ESR measurement at the oxidation wave of the compound has ravealed a well-resolved spectrum due to the cation redical. Although the reversibility of the first oxidation wave of all the other AOB's is less than that of 4,4′-bis(dimethylamino)-AOB mentioned above, the $E^{\rm oxd}_{1/2}$ values were determined by the wave analysis as reasonably as possible. All the data are included in Table 2.

Molecular Orbital (MO) Calculation and the Character of the Electronic Spectra. Some qualitative discussions of the excited states of AOB's have previously been reported,[2-6] but there have been no systematic considerations of their electronic states. In order to interpret the electronic spectra and their correlation with the $E^{\rm red}_{1/2}$ and $E^{\rm oxd}_{1/2}$ values, we have carried out the so-called PPP-SCFMO-CI calculations of the AOB's. As has been discussed in the "Electronic Spectra" section, the spectrum of AOB is quite similar to that of BANO (a nitrone). Since the electronic structures of nitrones including BANO were previously studied in detail,[16] the electronic states of AOB's may reasonably be understood by replacing the carbon atom in the bridge part of nitrones with a nitrogen atom, whose valence-state ionization potential ($I_{\rm P}$: 14.51) and electron affinity ($E_{\rm A}$: 1.20) are taken for the π electron in sp^2 hybridization.[20] The substituents employed in the calculations are the CH_3, Cl, OCH_3, and $N(CH_3)_2$ groups, the $I_{\rm P}$, $E_{\rm A}$, and core resonance energy ($\beta^{\rm core}_{\rm XY}$) of which are the same as those reported in a foregoing paper.[1d] The benzene ring in AOB was assumed to be a regular hexagon with the distance of 1.384 Å, cited from the X-ray analysis data of substituted AOB's.[17a]

The $\beta^{\rm core}_{\rm XY}$ values in the bridge part, *i.e.*, $\beta^{\rm core}_{\rm C-N}$ and $\beta^{\rm core}_{\rm N=N}$, were evaluated as follows. The $\beta^{\rm core}_{\rm CN}$ was estimated by applying the Nishimoto and Forster equation,[21] $\beta^{\rm core}_{\rm CN}=-0.53P_{\rm CN}-2.24$, where the bond order, $P_{\rm CN}$, was calculated from the $R_{\rm CN}=1.451-0.18P_{\rm CN}$ relation and where the observed CN distance, $R_{\rm CN}=1.496$ Å.[17a] The obtained value is $\beta^{\rm core}_{\rm CN}=-2.108$ eV. Alternatively, the value of $\beta^{\rm core}_{\rm N=N}$ tentavively estimated by employing the various equations connecting the $\beta^{\rm core}_{\mu\nu}$, $S_{\mu\nu}$, valence state $I_{\rm P}$, *etc.* led to the conclusion

TABLE 3. CALCULATED VALUES OF TRANSITION ENERGIES, OSCILLATOR STRENGTHS, AND MAIN SINGLY EXCITED CONFIGURATIONS OF AZOXYBENZENE AND BENZALDEHYDE *N*-PHENYL OXIME, WITH THEIR EXPERIMENTAL DATA

Compound	$\tilde{\nu}_{\rm calcd}$ (10^3 cm^{-1})	$f_{\rm calcd}$	$\tilde{\nu}_{\rm obsd}$[a] (10^3 cm^{-1})	$\varepsilon_{\rm max}$[a]	Main configuration (%)[b]
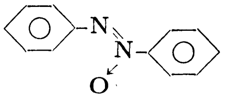	30.28	0.679	31.10	16050	92.6(8/9)
	33.63	0.064			77.8(7/9), 12.9(8/12)
	35.89	0.044			76.2(6/9), 13.8(5/10)
	38.65	0.261	38.94	7945	93.9(5/9)
	42.09	0.038	43.09	10180	56.1(8/12), 15.2(7/13), 13.9(7/9)
	44.09	0.050			78.0(4/9)
	45.90	0.027			76.6(8/11)
	46.43	0.081			39.5(8/10), 19.9(6/11), 17.0(6/9)
	47.57	0.012			55.8(8/10), 29.3 (5/10)
	50.06	0.134	50.61	27520	35.1(8/13), 30.8(7/12), 10.9(8/11)
	51.20	0.175			57.2(6/10), 24.8(5/11)
	53.54	0.670	53.25	35340	27.7(7/13), 26.0(7/11), 19.8(7/12)
	54.44	0.905			29.8(7/12), 28.7(8/13)
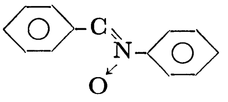	29.76	0.666	31.14	18600	97.5(8/9)
	34.66	0.007			61.7(7/9), 26.6(8/12)
	37.36	0.040			61.8(5/9), 13.9(6/10)
	38.94	0.398			85.8(6/9)
	41.42	0.004	41.25	11500	73.0(8/11), 17.0(8/12)
	42.13	0.000	42.05	11800	84.2(8/10)
	42.47	0.266	44.58	8540	46.4(8/12), 25.3(7/9), 12.9(8/11)
	43.60	0.011			80.8(4/9)
	48.09	0.018			41.7(6/10), 21.3(8/13), 16.7(5/9)
	48.89	0.253	51.33	32300	46.7(8/13), 12.9(7/12), 11.2(5/11)
	51.16	0.321			64.5(5/10), 23.1(6/11)
	53.10	0.803			62.6(7/12), 12.7(8/13)

a) All the experimental data are in heptane. See Ref. 16 for the spectral data of benzaldehyde *N*-phenyl oxime (BANO). b) For example, (8/9) means a singly excited configuration from ϕ_8 to ϕ_9.

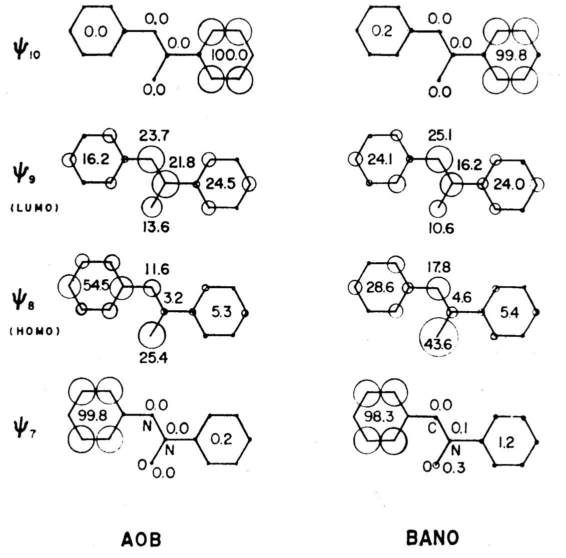

Fig. 5. Comparison of the orbital charge distributions, which are pertinent to the longer wavelength absorption bands, between azoxybenzene and benzaldehyde *N*-phenyl oxime.

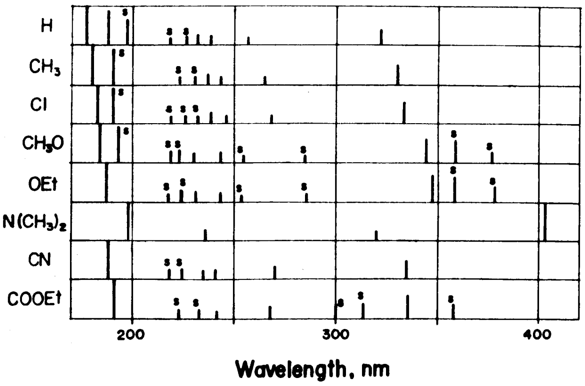

Fig. 6. Effect of substituents at *p,p'*-positions on the electronic spectra of azoxybenzene. The "s" in the figure means the shoulder band.

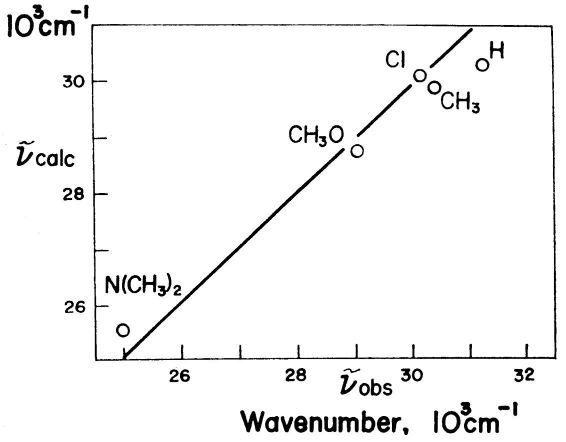

Fig. 7. Mutual correlation of calculated and observed values for the first strong π-π* band of *p,p'*-disubstituted azoxybenzenes.

that the $\beta_{N=N}^{core}$ is in the range 2.00—3.00 eV. With this result in mind, the $\beta_{N=N}^{core}=2.75$ eV was the most suitable for reproducing the observed UV spectra and dipole moments of AOB's.[22] The N atoms in the -N=N(O)- bridge group are assumed to be in sp^2 hybridization, so that the angles of ∠CNN and ∠CNO are 120° in the *trans*-form, as is shown in [I]. Here, one-electron transitions alone were taken into account in the UV spectral calculation. The excited-state energies of AOB are illustrated in Fig. 1 as stick diagram, while all the calculated and experimental spectral data on it are collected in Table 3, where the corresponding data of BANO are included for the sake of comparison. The orbital electron densities pertinent to the UV spectra are also shown in Fig. 5 for AOB and BANO. It is clear from Table 3 that the strong band of AOB (≈321.5 nm) and that (≈321.1 nm) of BANO appearing in the longest-wavelength region are mainly contributed by the HOMO→LUMO transition. This conclusion is the same as that reported hitherto by other workers;[2-6] their discussions were, however, in the framework of HOMO, without any CI treatment. The tentative assignment of the other bands of AOB and BANO is indicated in Table 3. Quite a good similarity is observed between the two calculations, which may suggest that the two bands recorded at 256.8 and ≈232.1 nm on AOB are coagulated into one band (263—224 nm) for BANO. The orbital-charge distribution (25.4%) on the *N*-oxide group oxygen atom in the HOMO of AOB is much less than that (43.6%) of BANO, so the charge-transfer (CT) character[24] from the above oxygen atom to the π-residual system is also smaller for AOB than in BANO for the case of the HOMO→LUMO transition (the strong band at ≈322 nm). For AOB, this transition is, rather, considered to be an intramolecular CT from the A ring to the bridge N=N(O) group and to the B ring (see Fig. 5 and [I]).[26]

Let us now focus our attention on the substituent effect on the spectrum of AOB. As may be seen in Table 2 and Fig. 6, the first strong π-π* band is quite sensitive to the 4,4'-substituents with an electron-donor nature, and shows a red shift which is particularly large for the $N(CH_3)_2$ group. This result was confirmed by the present MO calculation, as Fig. 7 shows. The calculation indicates that the first strong π-π* band observed on the 4,4'-substituted AOB's is also contributed mainly by the HOMO→LUMO transition. On the other hand, the shift of the first strong π-π* band is small for the case of *m,m'*-substitution of AOB. The results, listed in Table 2, may be explained qualitatively as follows. The MO coefficients of AOB at the *m,m'*-positions are quite small (see Fig. 5) for the HOMO and LUMO, which contribute greatly to the above π-π* band. Therefore, the small perturbation of these orbitals can be expected from the introduction of *m,m'*-substituents, leading to the small spectral shift. The red shift of the spectra of AOB's due to the solvent change from heptane to protic solvents was described in the foregoing section. The general rule pertaining to the blue-shift phenomena[27] caused by the solvent effect on the electronic spectra of aromatic tertiary amine *N*-oxides seems not to hold for AOB's.[28] That the first strong π-π* band of AOB is somewhat different in CT nature from that of BANO has already been discussed. This tendency increases with, for example, an increasing electron-donor nature of the substituents introduced at 4,4′-positions. For 4,4′-$(OCH_3)_2$ or 4,4′-$[N(CH_3)_2]_2$, the electron densities on the *N*-oxide-group oxygen atom are quite small at HOMO (14.36 and 6.33% for the former and the latter respectively), so there is almost no CT from the oxygen atom to the π-residual system in the case of the HOMO→LUMO transition. On the other hand, the electron densities at the N(8) atom (see [I]) always increased upon the HOMO→LUMO transition. These circumstances would be favorable to the red shift of the π-π^* band in protic solvents; that is, such intermolecular interactions as hydrogen bonding with protic solvents would become more or less stronger in the excited π-π^* state than in the ground state.

The Correlation of the Electronic Spectra and Half-wave Potentials. The fact that the first strong π-π^* band of substituted AOB's at the 4,4′-positions is mainly contributed by the HOMO→LUMO transition has been shown in the previous chapter. The linear relation written as Eq. 1 can thus be expected for the AOB's:

$$(E_{1/2}^{\text{oxd}}-E_{1/2}^{\text{red}}) = k_1\cdot{}^1E_{\text{ho}\to\text{lu}}^{\text{UV}} + k_2 \qquad (1)$$

Here, ${}^1E_{\text{ho}\to\text{lu}}^{\text{UV}}$ is the singlet electronic transition energy, in which the HOMO→LUMO transition is the main configuration.[30] Of course, if the configuration of triplet excited states (${}^3E_{\text{ho}\to\text{lu}}^{\text{UV}}$) is localized mainly in the HOMO→LUMO transition, Eq. 2 can also be expected:

$$(E_{1/2}^{\text{oxd}}-E_{1/2}^{\text{red}}) = k_1\cdot{}^3E_{\text{ho}\to\text{lu}}^{\text{UV}} + k_3 \qquad (2)$$

This relation was recently observed by Loutfy and Loutfy.[31] Figure 8 gives the correlation of Eq. 1, each of the experimental data being taken from Table 2. A good linear relation is found there for 4,4′-substituents, as is to be expected from the MO calculation.[32] The observed k_1 value is 1.27, which is near the theoretical value, 1. Alternatively, the k_2 value of -1.44 was obtained. In the case of the *m,m′*-substituents, the shift of the UV spectra is insensitive even to the groups of a stronger electron-donor or -acceptor, as may be seen in Fig. 3 so that the correlation of Eq. 1 was not obtained. The character of the absorption bands for these substances seems to be somewhat different from those of 4,4′-substituents. For the physical meaning of the k_2 and k_3 terms in Eq. 1 or 2, see the Appendix.

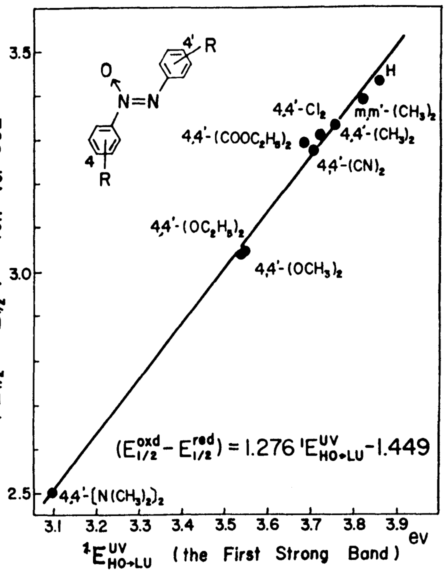

Fig. 8. The relationship between $(E_{1/2}^{\text{oxd}}-E_{1/2}^{\text{red}})$ values and the first strong π-π^* band energies for 4,4′-disubstituted azoxybenzenes.

Substituent Effect on the $E_{1/2}^{\text{oxd}}$ and $E_{1/2}^{\text{red}}$ values. In a previous paper we have already pointed out that, in the electrode oxidation process, the σ^+ substituent constant is the better parameter to explain the substituent effect on the $E_{1/2}^{\text{oxd}}$ values.[7a)] On the other hand, the usual σ or σ^- scales afford a better description of the substituent effect on the $E_{1/2}^{\text{red}}$ values.[8,33)] In the series of AOB's these same relationships have also been observed. The plotting of the $E_{1/2}^{\text{oxd}}$ values against the $2\sigma^+$ gave a nice linear relation, as is indicated in Fig. 9.[34)] In the case of the $E_{1/2}^{\text{red}}$ values, the good linearity shown in Fig. 10 was also found for 2σ and partly $2\sigma^-$ parameters; σ^- values were adopted for 4,4′-$(NO_2)_2$, 4,4′-$(CN)_2$, and 4,4′-$(COOC_2H_5)_2$, because the electron-accepting ability in the transition state is large for these. The above fact indicates that the treatment of a linear free-energy approximation can safely be applied to the half-wave potentials of AOB's in nonaqueous media, and that

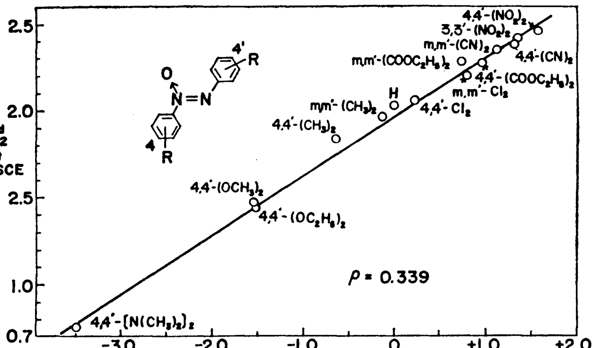

Fig. 9. Linear relationship between the σ^+ values (see Table 2) and the first $E_{1/2}^{\text{oxd}}$ values for substituted azoxybenzenes.

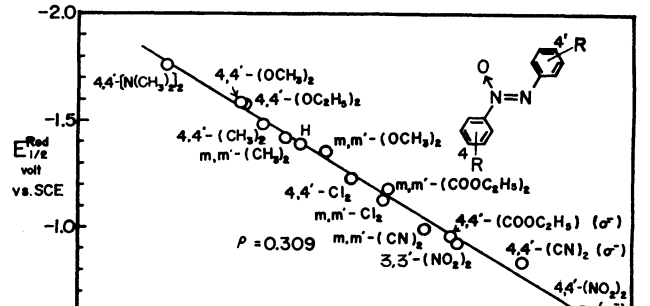

Fig. 10. Linear relationship between the σ and σ^- values (see Table 2) and the first $E_{1/2}^{\text{red}}$ values for substituted azoxybenzenes.

the above-mentioned linear relations make it easy to predict the $E^{\mathrm{red}}_{1/2}$ and $E^{\mathrm{oxd}}_{1/2}$ of substituted AOB's.

Appendix

In our previous papers[7] we did not discuss quantitatively the physical meaning of the constant terms, k_2 and k_3, in Eqs. 1 and 2 respectively. Here an interpretation of the k_2 and k_3 terms will be given. Let us now consider a reversible system of anion-radical formation, such as $\mathrm{R}+\mathrm{e}\rightleftarrows\mathrm{R}^{\dot{-}}$, so that the k_1 value of Eqs. 1 and 2 becomes 1 when the electron volt (eV) is adopted as the energy unit.[36] Applying the Born-Haber-type[35] thermochemical cycle given in Scheme 1 for anion-radical formation in solution, the $E^{\mathrm{red}}_{1/2}$ $(\mathrm{R}^{\dot{-}}/\mathrm{R})$ can be written by Eq. 3 in eV units, where the energy zero level is placed *in vacuo*:[31,37]

$$E^{\mathrm{red}}_{1/2}(\mathrm{R}^{\dot{-}}/\mathrm{R}) = \Delta G^{\circ} - \varepsilon_{\mathrm{lu}} - \Delta E^{\dot{-}}_{\mathrm{solv}} \tag{3}$$

$$\begin{tikzcd}
\mathrm{R} \arrow[r, "+\mathrm{e}", "\substack{\text{in gas phase}\\(-E_{\mathrm{A}}=\varepsilon_{\mathrm{lu}})}"'] \arrow[d, "E^{\mathrm{R}}_{\mathrm{solv}}"'] & \mathrm{R}^{\dot{-}} \\
\mathrm{R}_{\mathrm{solv}} \arrow[r, "\text{in solution}", "F\cdot E^{\mathrm{red}}_{1/2}(\mathrm{R}^{\dot{-}}/\mathrm{R})"'] & \mathrm{R}^{\dot{-}}_{\mathrm{solv}} \arrow[u, "-E^{\mathrm{R}^{\dot{-}}}_{\mathrm{solv}}"']
\end{tikzcd}$$

Scheme 1.

$\Delta E^{\dot{-}}_{\mathrm{solv}}$ is the solvation energy difference of the anion radical and neutral species; $\Delta E^{\dot{-}}_{\mathrm{solv}}=E^{\mathrm{R}^{\dot{-}}}_{\mathrm{solv}}-E^{\mathrm{R}}_{\mathrm{solv}}$. The contribution from the $E^{\mathrm{R}^{\dot{-}}}_{\mathrm{solv}}$ term is predominant. The absorolute potential of the reference electrode is expressed as ΔG°, which is -4.70 eV in the case of the ($\mathrm{Ag/Ag^+}$) electrode in acetonitrile (0.01 mol dm^{-3} $\mathrm{AgClO_4}$, 0.1 mol dm^{-3} $\mathrm{Et_4N^+ClO_4^-}$).[37] Similarly the $E^{\mathrm{oxd}}_{1/2}(\mathrm{R}^{\dot{+}}/\mathrm{R})$ is given by:

$$E^{\mathrm{oxd}}_{1/2}(\mathrm{R}^{\dot{+}}/\mathrm{R}) = \Delta G^{\circ} - \varepsilon_{\mathrm{ho}} + \Delta E^{\dot{+}}_{\mathrm{solv}} \tag{4}$$

The $\Delta E^{\mathrm{R}\dot{+}}_{\mathrm{solv}}$ equals $(E^{\dot{+}}_{\mathrm{solv}}-E^{\mathrm{R}}_{\mathrm{solv}})$. Taking account of the difference between Eqs. 3 and 4, Eq. 5 is obtained under the same experimental conditions, *i.e.*, the ΔG° term is cancelled out:[38]

$$(E^{\mathrm{oxd}}_{1/2}-E^{\mathrm{red}}_{1/2}) = \varepsilon_{\mathrm{lu}} - \varepsilon_{\mathrm{ho}} + \Delta E^{\dot{+}}_{\mathrm{solv}} + \Delta E^{\dot{-}}_{\mathrm{solv}} \tag{5}$$

Note that the $(E^{\mathrm{oxd}}_{1/2}+E^{\mathrm{red}}_{1/2})/2\approx E^{\circ}(\mathrm{R}^{\dot{-}}/\mathrm{R}^{\dot{+}})$ may become $(-\varepsilon_{\mathrm{ho}}-\varepsilon_{\mathrm{lu}})/2+\Delta G^{\circ}=(I_{\mathrm{P}}+E_{\mathrm{A}})/2+\Delta G^{\circ}$ when we use Eqs. 3 and 4 and $\Delta E^{\dot{-}}_{\mathrm{solv}}=\Delta E^{\dot{+}}_{\mathrm{solv}}$. This relation was employed by Senda and Takahashi to determine the standard electrode potential in nonaqueous solvents.[37b,49] We will now combine Eq.5 with this relation: ${}^1E^{\mathrm{UV}}_{\mathrm{ho}\to\mathrm{lu}}=\varepsilon_{\mathrm{lu}}-\varepsilon_{\mathrm{ho}}-J_{\mathrm{ho\cdot lu}}+2K_{\mathrm{ho\cdot lu}}+{}^1E_{\mathrm{CI}}$, where the small contribution from the CI energy (${}^1E_{\mathrm{CI}}$) is postulated.[7] Thus, the k_2 value in Eq. 1 is given by Eq. 6 in eV units for a completely reversible system:

$$\begin{aligned} k_2 &= J_{\mathrm{ho\cdot lu}} - 2K_{\mathrm{ho\cdot lu}} - {}^1E_{\mathrm{CI}} + \Delta E^{\dot{-}}_{\mathrm{solv}} + \Delta E^{\dot{+}}_{\mathrm{solv}} \\ &\approx J_{\mathrm{ho\cdot lu}} - 2K_{\mathrm{ho\cdot lu}} - {}^1E_{\mathrm{CI}} + 2\Delta E^{\dot{-}}_{\mathrm{solv}} \end{aligned} \tag{6}$$

Similarly, the k_3 value in Eq. 2 is given by

$$\begin{aligned} k_3 &= J_{\mathrm{ho\cdot lu}} - {}^3E_{\mathrm{CI}} + \Delta E^{\dot{-}}_{\mathrm{solv}} + \Delta E^{\dot{+}}_{\mathrm{solv}} \\ &\approx J_{\mathrm{ho\cdot lu}} - {}^3E_{\mathrm{CI}} + 2\Delta E^{\dot{-}}_{\mathrm{solv}} \end{aligned} \tag{7}$$

Recently Loutfy and Loutfy discussed the meaning of the k_2 and k_3 values.[31] However, they completely neglected the term of $(\Delta E^{\dot{-}}_{\mathrm{solv}}+\Delta E^{\dot{+}}_{\mathrm{solv}})$. In addition, their MO's participating in the UV transition, which they interpreted as the "molecular orbital in solution" of neutral species, should rather be ascribed to those of the anion and cation radicals (${}^2\Gamma$ state) generated by electrolysis. Also, they used the $E^{\mathrm{red}}_{1/2}$ and $E^{\mathrm{oxd}}_{1/2}$ values obtained in different solvents ($\mathrm{CH_3CN}$ and DMF) for plotting Eqs. 1 and 2 in the case of AH hydrocarbons, so the $(\Delta G^{\circ}_{\mathrm{CH_3CN}}-\Delta G^{\circ}_{\mathrm{DMF}})$ term should appear in Eq. 5. They did not take care in this point. Their discussions, therefore, are erroneous.

In the case of the AH hydrocarbons there are some experimental data by which to estimate the k_2 and k_3 values. In addition, the fact that the k_1 value of Eq. 1 is experimentally almost 1 has already been reported.[7] The $\Delta E^{\dot{-}}_{\mathrm{solv}}$ and $\Delta E^{\dot{+}}_{\mathrm{solv}}$ values can be estimated from Eqs. 3 and 4 respectively by adopting the experimentally determined I_{P}, E_{A}, $E^{\mathrm{red}}_{1/2}$, and $E^{\mathrm{oxd}}_{1/2}$ values.[37] In turn, the value of $(J_{\mathrm{ho\cdot lu}}-2K_{\mathrm{ho\cdot lu}}-{}^1E_{\mathrm{CI}})$ can be experimentally derived from the evaluation of the $(I_{\mathrm{P}}-E_{\mathrm{A}}-{}^1E^{\mathrm{UV}}_{\mathrm{ho}\to\mathrm{lu}})$ value. The ${}^1\mathrm{L_a}$ bands of AH's correspond to the ${}^1E^{\mathrm{UV}}_{\mathrm{ho}\to\mathrm{lu}}$ value.[7] Here note that, in the foregoing papers,[7] we discussed how the value of the $(J_{\mathrm{ho\cdot lu}}-2K_{\mathrm{ho\cdot lu}}-{}^1E_{\mathrm{CI}})$ term becomes nearly constant from the standpoint of the PPP-SCFMO-CI calculation in a series of similar com-

TABLE 4. THE k_2 AND k_3 VALUES THEORETICALLY ESTIMATED ON THE ALTERNATE HYDROCARBONS, WITH SOME PHYSICAL CONSTANTS (see text) NECESSARY FOR DERIVING THE k_2 AND k_3 VALUES

Compound	$-E^{\mathrm{red}}_{1/2}$ (V)[a]	$E^{\mathrm{oxd}}_{1/2}$ (V)[a]	I_{P} (eV)[b]	E_{A} (eV)[c]	${}^1\mathrm{L_a}$ (eV)[d]	k^{theo}_2 (eV)[g,i]	${}^3\mathrm{L_a}$ (eV)	k^{theo}_3 (eV)[h,i]
Anthracene	2.37	0.99	7.66 7.47	0.552	3.310	0.05	1.838[e]	1.522
Pyrene	2.49	1.12	7.72 7.41	0.579	3.718	−0.108	2.083[e]	1.527
Chrysene	2.73	1.29	8.01 7.60	0.419	3.886	0.134	2.455[e]	1.565
Phenanthrene	2.88	1.45	8.06 7.86	0.288	4.238	0.082	2.689[f]	1.631
Benz[*a*]anthracene	2.40	1.16	7.74 7.47	0.696	3.491	0.069	2.050[f]	1.510
Triphenylene	2.87	1.50	8.19 7.89	0.284	4.365	0.005	2.907[f]	1.463
						0.039 ±0.083		1.551 ±0.057

a) Taken from Ref. 37a. b) Taken from Refs. 37a, 37b, and 40. c) Taken from Refs. 37b and 41. d) Taken from Refs. 7b and 42. e) Taken from Ref. 43. f) Taken from Ref. 44. g) The constant term in Eq. 1 in the test. h) The constant term in Eq. 2 in the text. i) The k_2 or k_3 value listed for each compound was obtained by averaging the values derived from the two different I_{P}'s.

pounds such as AH's or aromatic *N*-oxides.[48] The same treatment as the above leads to the evaluation of the $(J_{\text{ho}\cdot\text{lu}}-{}^3E_{\text{CI}})$ term, which is obtained from the calculation of $(I_\text{P}-E_\text{A}-{}^3E^{\text{UV}}_{\text{ho}\to\text{lu}})$. Here, ${}^3E^{\text{UV}}_{\text{ho}\to\text{lu}}$ is for the ${}^3\text{L}_\text{a}$ bands. We can now obtain the k_2 and k_3 values in Eqs. 6 and 7 respectively from the experimental values alone. The results thus obtained are listed in Table 4, from which it may be understood that the k_2 value is $\approx$0.04 eV and quite small, while the k_3 value is $\approx$1.55 eV. The $E^{\text{red}}_{1/2}$ and $E^{\text{oxd}}_{1/2}$ values in Table 4 are those reported under the same conditions as were used for the determination of $\Delta G^\circ=-4.70$ eV,[37] so these are the best values for the evaluation of k_2 and k_3. The plotting of Eqs. 1 and 2 was as follows: $(E^{\text{oxd}}_{1/2}-E^{\text{red}}_{1/2})=1.011\ {}^1\text{L}_\text{a}-0.001$ with $n=6$, $s=0.094$, $r=0.980$, and $(E^{\text{oxd}}_{1/2}-E^{\text{red}}_{1/2})=1.018\ {}^3\text{L}_\text{a}+1.496$ with $n=6$, $s=0.067$, $r=0.990$.[39] Note that our previously reported result[7b,c] was $(E^{\text{oxd}}_{1/2}-E^{\text{red}}_{1/2})=0.941\ {}^1\text{L}_\text{a}+0.092$. The values of the constant term given above seem to be in good agreement with the ones estimated theoretically in the order of magnitude and in the approximation adopted. For AOB's we did not attempt to evaluate the k_2 term in Eq. 1 because of the lack of experimental data and because of the smaller reversibility of the $E^{\text{red}}_{1/2}$ and, especially, $E^{\text{oxd}}_{1/2}$ values.

References

1) a) J. Bastide, J. P. Maier, and T. Kubota, *J. Electron Spectrosc.*, **9**, 307 (1976); b) M. Yamakawa, T. Kubota, K. Ezumi, and Y. Mizuno, *Spectrochim. Acta*, **30**, 2103 (1974); c) K. Ezumi, T. Kubota, and T. Shida, *Chem. Lett.*, **1977**, 181; d) M. Yamakawa, K. Ezumi, Y. Mizuno, and T. Kubota, *Bull. Chem. Soc. Jpn.*, **47**, 2982 (1974); e) Y. Kawamura, K. Nishikida, and T. Kubota, *Bull. Chem. Soc. Jpn.*, **46**, 737 (1973), and other articles listed in the above papers.

2) a) W. Maier and A. Saupe, *Z. Phys. Chem., N. F.*, **6**, 327 (1956); b) W. Maier, A. Saupe, and A. Englert, *Z. Phys. Chem., N. F.*, **10**, 273 (1957); c) W. Maier and G. Englert, *Z. Elektrochem.*, **62**, 1020 (1958); d) A. Saupe, *Z. Naturforsch., Teil A*, **18**, 336 (1963).

3) P. H. Gore and O. H. Wheeler, *J. Am. Chem. Soc.*, **78**, 2160 (1956).

4) a) D. L. Webb and H. H. Jaffé, *J. Am. Chem. Soc.*, **86**, 2419 (1964); b) H. H. Jaffé and M. Orchin, "Theory and Application of Ultraviolet Spectroscopy," John Wiley and Sons, (1962).

5) C. Tosi, *Spectrochim. Acta*, **22**, 1701 (1966).

6) The discussions in Refs. 2—5 are based on the naive MO approximation.

7) a) H. Miyazaki, T. Kubota, and M. Yamakawa, *Bull. Chem. Soc. Jpn.*, **45**, 780 (1972); b) T. Kubota, H. Miyazaki, K. Ezumi, and M. Yamakawa, *Bull. Chem. Soc. Jpn.*, **47**, 491 (1974); c) T. Kubota and H. Miyazaki, *Bunseki Kiki*, **11**, 639 (1973).

8) T. Kubota, K. Nishikida, H. Miyazaki, K. Iwatani, and Y. Ōishi, *J. Am. Chem. Soc.*, **90**, 5080 (1968).

9) K. Nishikida, T. Kubota, H. Miyazaki, and S. Sakata *J. Magn. Reson.*, **7**, 260 (1972).

10) A. McKillop, R. A. Raphael, and E. C. Taylor, *J. Org. Chem.*, **35**, 1670 (1970).

11) J. F. Corbett, *Chem. Commun.*, **1968**, 1257.

12) W. H. Linnell and M. Khalifa, *J. Chem. Soc.*, **1959**, 1315.

13) T. Kubota and H. Watanabe, *Bull. Chem. Soc. Jpn.*, **36**, 1093 (1963).

14) a) K. E. Calderbauk and R. J. W. LeFévre, *J. Chem, Soc.*, **1948**, 1949; b) R. A. Gehrchevs and E. Müller, *Ann.*, **500**, 296 (1933).

15) T. Shimozawa, "Interpretation of Dielectric Behavior (Experimental Method of Dipole Moment and Its Interpretation)," Kyōritsu Press, Tokyo (1967), p. 55 (in Japanese).

16) The electronic spectra and their interpretation of various nitrones have already been reported in detail. a) T. Kubota, M. Yamakawa, and Y. Mori, *Bull. Chem. Soc. Jpn.*, **36**, 1552 (1963); b) T. Kubota and M. Yamakawa, *Bull. Chem. Soc. Jpn.*, **36**, 1564 (1963); c) M. Yamakawa, T. Kubota, and H. Akazawa, *Theor. Chim. Acta*, **15**, 244 (1969); d) J. Bastide, J. P. Maier, and T. Kubota, *J. Electron Spectrosc. Relat. Phenom.*, **9**, 307 (1976); e) K. N. Houk, P. Caramella, L. L. Munchausen, Y-M. Chang, A. Battaglia, J. Sims, and D. C. Kaufman, *J. Electron. Spectrosc. Relat. Phenom.*, **10**, 441 (1977).

17) See the following papers on the molecular structure of azoxybenzenes; a) W. R. Krigbaum, Y. Chatani, and P. G. Barber, *Acta Crystallogr., Sect. B*, **26**, 97 (1970); b) W. R. Krigbaum and P. G. Barber, *Acta Crystallogr., Sect. B*, **27**, 1884 (1971).

18) N. Mataga and T. Kubota, "Molecular Interactions and Electronic Spectra," Marcel Dekker, New York (1970), Chap. 8.

19) Just before the use of the Pt-electrode the plane platinum head was polished with very fine emery paper; therefore, the reproducibility of the AC wave was good. See also Ref. 7a.

20) a) G. Pilcher and H. A. Skinner, *J. Inorg. Nucl. Chem.* **24**, 937 (1962); b) J. Hinze and H. H. Jaffé, *J. Am. Chem. Soc.*, **84**, 540 (1962).

21) K. Nishimoto and L. S. Forster, *Theo. Chim. Acta*, **4**, 155 (1966).

22) The parameters other than those written in the text are the same as in our previous reports.[1d,16c,23]

23) T. Kubota, M. Yamakawa, and Y. Mizuno, *Bull. Chem. Soc. Jpn.*, **45**, 3282 (1972).

24) This type of intramolecular CT is generally found in the case of aromatic amine oxides such as heterocyclic amine N-oxides, nitrones, and nitrile *N*-oxides.[1b,16,18,25]

25) T. Kubota, *Bull. Chem. Soc. Jpn.*, **35**, 946 (1962).

26) Quite recently a conclusion similar to this was reported on the basis of an INDO/S calculation of AOB; N. J. Bunce, J-P. Schoch, and M. C. Zerner, [*J. Am. Chem. Soc.*, **99**, 7986 (1977).

27) T. Kubota and H. Miyazaki, *Chem. Pharm. Bull.*, **9**, 948 (1961).

28) AOB itself shows a blue shift of 50 cm^{-1} alone from heptane to ethanol. Also, our experiments have revealed that the hydrogen-bonding interaction ability of AOB with phenol is $K=2$—5 dm^3 mol^{-1} in CCl_4 at 25 °C and that the shift of the phenol OH-stretching band is 174 cm^{-1} in CCl_4. Note that the shift of the methanol OH-stretching band brought about by the intermolecular hydrogen bonding with benzaldehyde *N*-methyl oxime (nitrone) is 238 cm^{-1} in CCl_4.[29] These findings indicate AOB to be much weaker a proton-acceptor in the ground state than in a nitrone such as BANO.[29]

29) a) T. Kubota, M. Yamakawa, M. Takasuka, K. Iwatani, H. Akazawa, and I. Tanaka, *J. Phys. Chem.*, **71**, 3597 (1967); b) T. Kubota, *J. Am. Chem. Soc.*, **88**, 211 (1966), and other papers cited in Ref. 29.

30) The derivation and the examination of Eq. 1 have already been reported elsewhere by us.[7] See also the Appendix for the physical meaning of the constant term (k_2) of Eq. 1.

31) Rafik O. Loutfy and Raouf O. Loutfy, *Can. J. Chem.*, **54**, 1454 (1976).

32) Although the MO calculation for the AOB substituted with 4,4′-$(CN)_2$ and 4,4′-$(COOC_2H_5)_2$ was not attempted, the first strong π-π^* band seems to be mainly contributed by the HOMO→LUMO transition, judging from our previous calculation of 4-nitropyridine *N*-oxide, *etc.*[1b]

33) T. Kubota and H. Miyazaki, *Bull. Chem. Soc. Jpn.*, **39**, 2057 (1966).

34) If the plotting is made for usual σ values, the linearity in Fig. 8 becomes quite bad, particularly for the strong electrondonating substituents.

35) L. Pauling, "The Nature of the Chemical Bond," 3rd ed, Cornell University Press, Ithaca, New York (1960), p. 510.

36) This is because the Faraday constant becomes 1 eV/1 V, so that in Eqs. 3, 4, and 5 in the text $F \cdot E_{1/2}$ is simply expressed by $E_{1/2}$.

37) a) B. Case, N. S. Hush, R. Parsons, and M. E. Peover, *J. Electroanal. Chem.*, **10**, 360 (1965); b) M. Senda and R. Takahashi, *Rev. Polarog. (Kyoto)*, **20**, 56 (1974); c) M. E. Peover, "Electroanalytic Chemistry," ed by A. J. Bard, Marcel Dekker, New York, N. Y. (1967), Vol. 2, Chap. 1; d) Rafik O. Loutfy and Raouf O. Loutfy, *J. Phys. Chem.*, **77**, 336 (1973).

38) In these equations the solvation energy of the ion radicals indicates the so-called "real solvation energy," which includes the energy term $F \cdot \chi$. Here χ is the surface potential caused by transferring the ion redical from the gas phase to the solvent phase, both the phases being electrically neutral. The χ value for CH_3CN may be expected to be small.[37a,c)]

39) Here, *n*, *s*, and *r* indicate the number of samples adopted for the least-squares calculation, the standard deviation, and the correlation coefficient respectively.

40) R. Boschi, E. Clar, and W. Schmidt, *J. Chem. Phys.*, **60**, 4406 (1974).

41) a) W. E. Wentworth, E. Chen, and J. E. Lovelock, *J. Phys. Chem.*, **70**, 445 (1966); b) W. E. Wentworth, L. W. Kao, and R. S. Becker, *J. Phys. Chem.*, **79**, 1161 (1975).

42) E. Clar, "Polycyclic Hydrocarbons," Academic Press, London (1964), Vols. 1 and 2.

43) S. P. McGlynn, T. Azumi, and M. Kinoshita, "Molecular Spectroscopy of the Triplet State," Prentice-Hall, Englewood Cliffs, New Jersey (1969).

44) P. S. Engel and B. M. Monroe, *Adv. Photochem.*, **8**, 245 (1971).

45) H. C. Brown and Y. Okamoto, *J. Am. Chem. Soc.*, **80**, 4979 (1958).

46) T. Kubota and H. Miyazaki, *Bull. Chem. Soc. Jpn.*, **39**, 2057 (1966).

47) a) H. H. Jaffé, *Chem. Revs.*, **53**, 191 (1953); b) M. Yoshioka, K. Hamamoto, and T. Kubota, *Bull. Chem. Soc. Jpn.*, **35**, 1723 (1962); c) C. Hansch, A. Leo, S. H. Unger, K-H. Kim, D. Nikaitani, and E. J. Lien, *J. Med. Chem.*, **16**, 1207 (1973); d) C. Hansch, S. D. Rockwell, P. Y. C. Jow, A. Leo, and E. E. Steller, *J. Med. Chem.*, **20**, 304 (1977).

48) In the present series, almost constant negative values of $\Delta E_{\mathrm{solv}}^{\dot{-}}$ and $\Delta E_{\mathrm{solv}}^{\dot{+}}$ were also obtained from Eqs. 3 and 4.

49) T. Kakutani, Y. Morihiro, M. Senda, R. Takahashi, and K. Matsumoto, *Bull. Chem. Soc. Jpn.*, **51**, 2847 (1978).

50) For this reason, the notation of *m,m'* is adopted in this report for the compounds whose accurate configurations in the *m,m'*-positions could not be determined.